

Electronic Supplementary Information

Thermally activated delayed fluorescence dendrimers with exciplex-forming dendrons for low-voltage-driving and power-efficient solution-processed OLEDs

Kaiyong Sun,^a Yibai Sun,^b Wenwen Tian,^a Dan Liu,^a Yingli Feng,^a Yueming Sun^{*a}
and Wei Jiang^{*a}

^a Jiangsu Engineering Laboratory of Smart Carbon-Rich Materials and Device, Jiangsu Province Hi-Tech Key Laboratory for Bio-Medical Research, School of Chemistry and Chemical Engineering, Southeast University, Nanjing, Jiangsu, 211189, P. R. China.

^b Department of Chemical and Pharmaceutical Engineering of Southeast University Chengxian College, Nanjing, Jiangsu, 210088, P. R. China

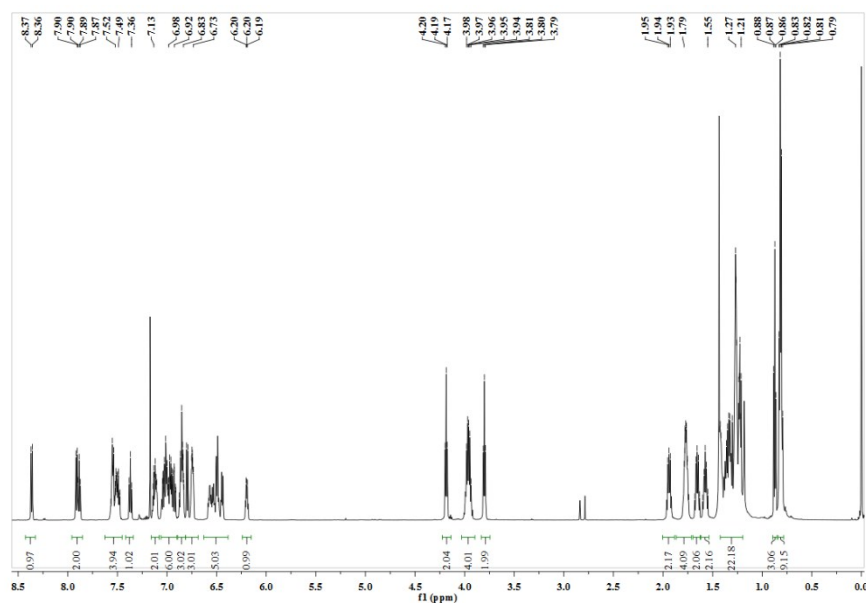


Fig. S1. ¹H NMR spectra of G-G0.

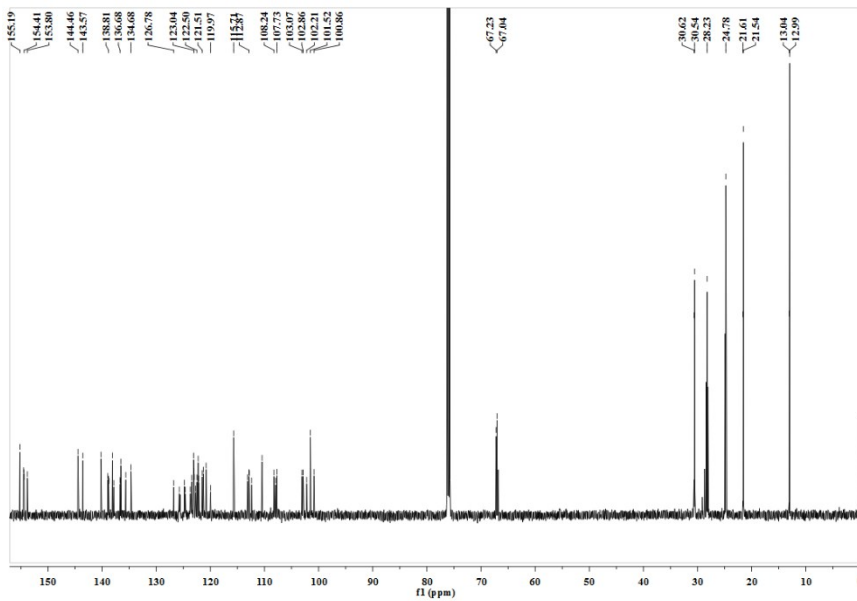


Fig. S2. ^{13}C NMR spectra of G-G0.

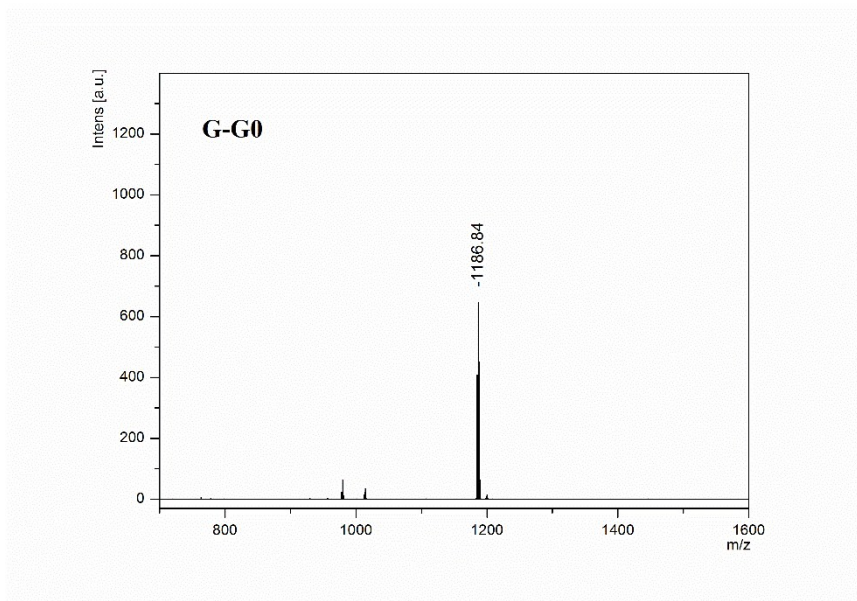


Fig. S3. MALDI-TOF-MS spectra of G-mCP.

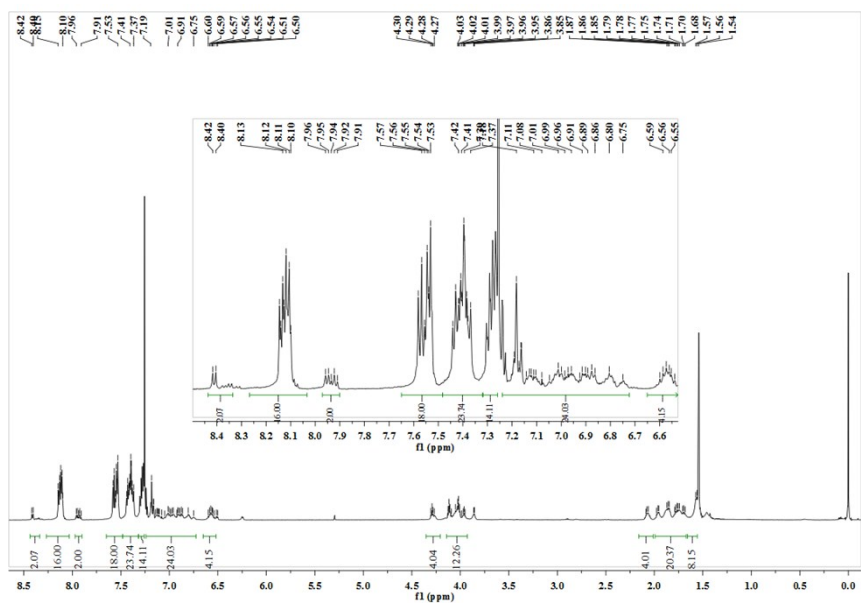


Fig. S4. ^1H NMR spectra of G-mCP.

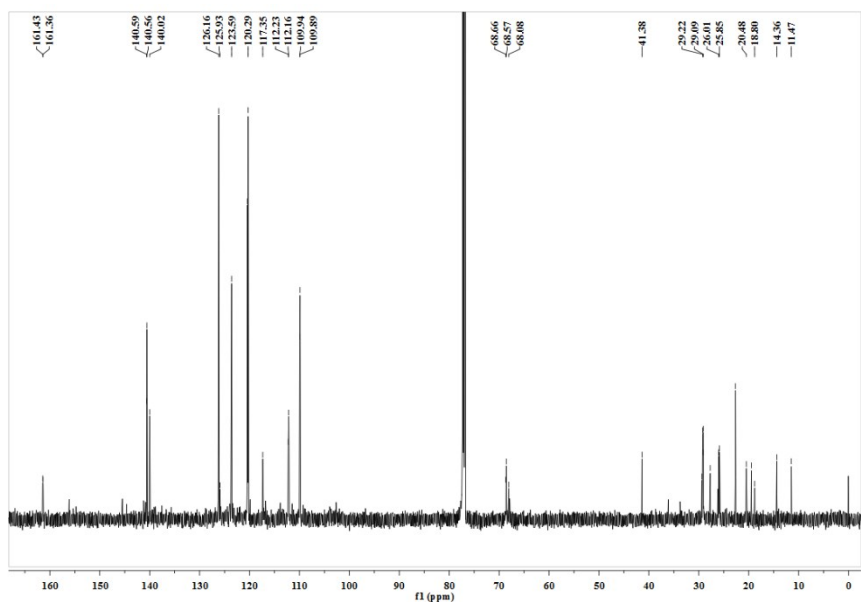


Fig. S5. ^{13}C NMR spectra of G-mCP.

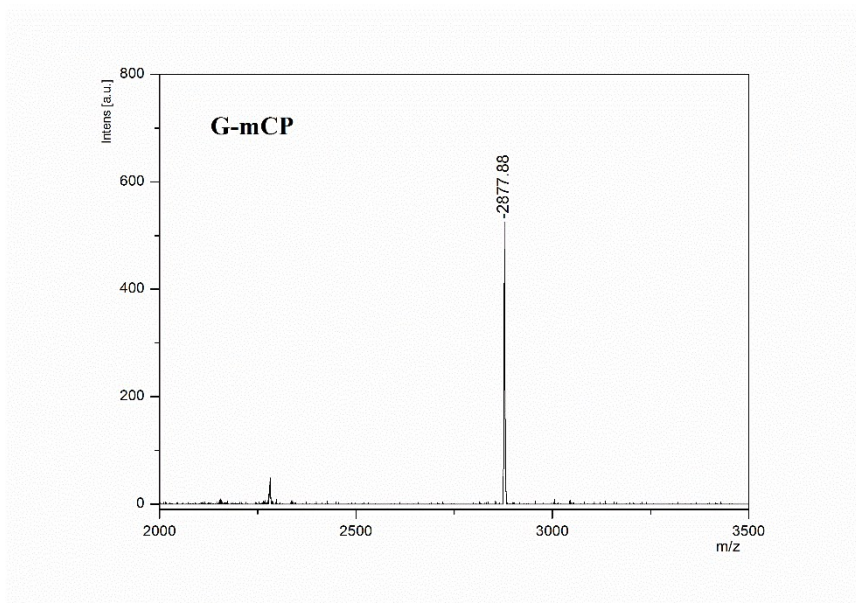


Fig. S6. MALDI-TOF-MS spectra of G-mCP.

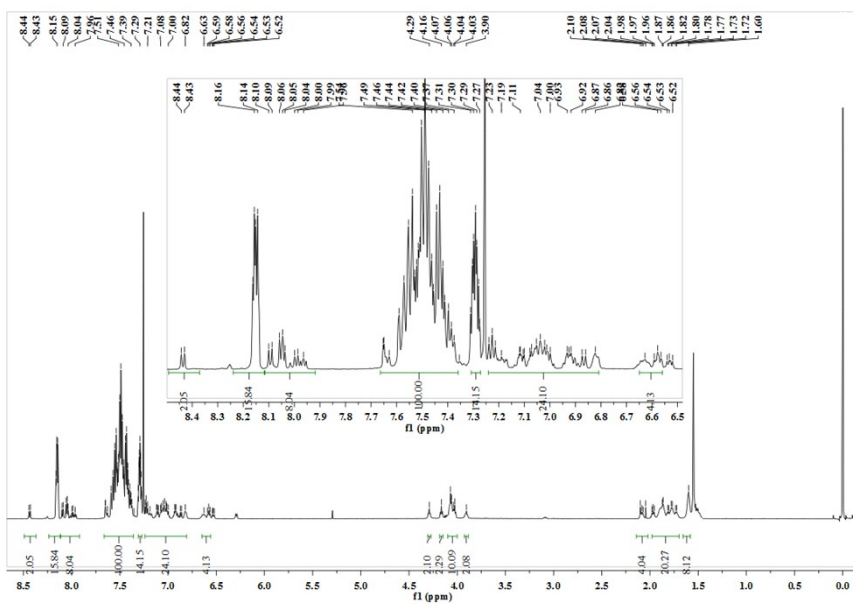


Fig. S7. ¹H NMR spectra of G-TCTA.

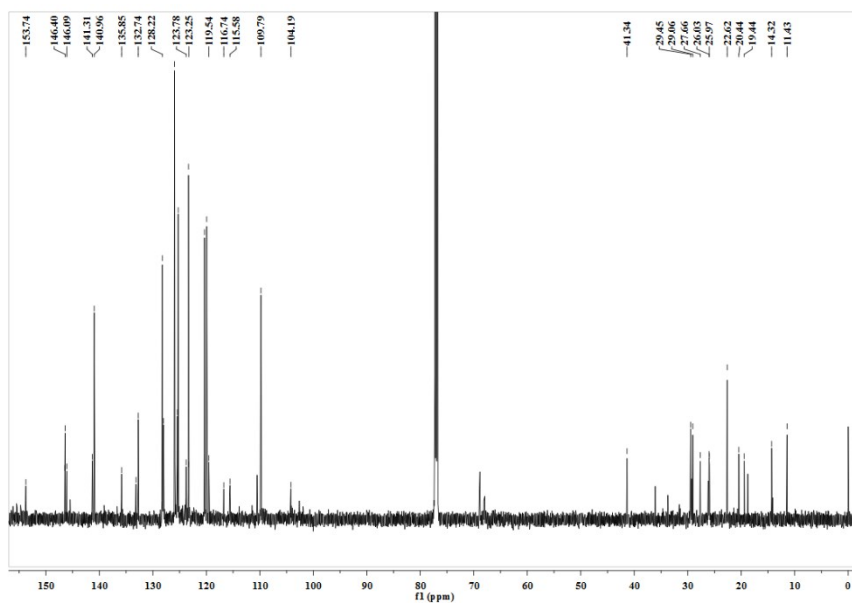


Fig. S8. ^{13}C NMR spectra of G-TCTA.

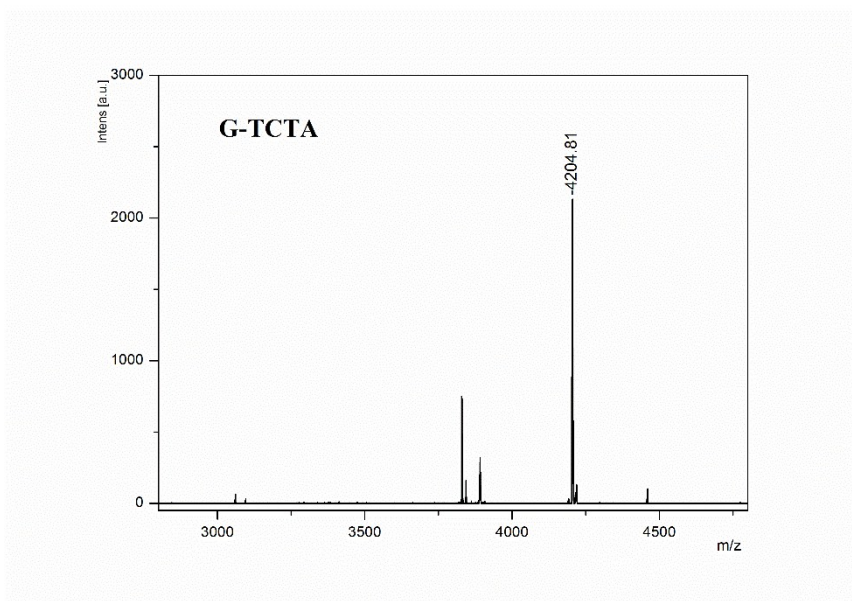


Fig. S9. MALDI-TOF-MS spectra of G-TCTA.

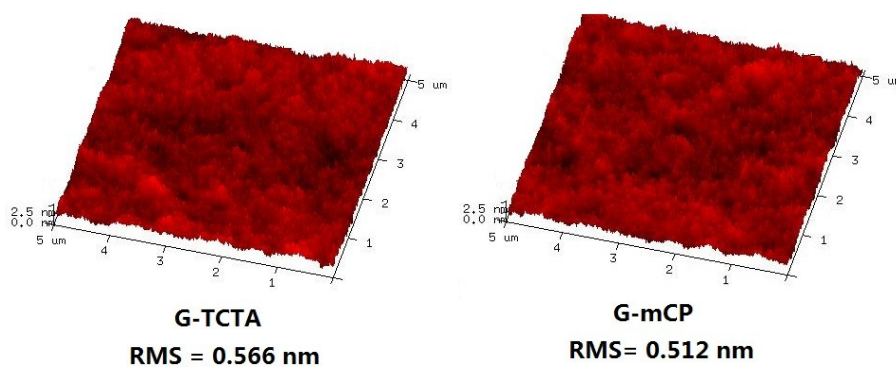
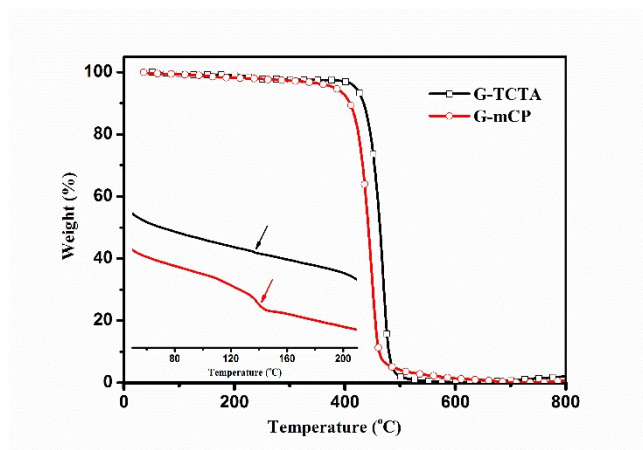


Fig. S10. (a) TGA and DSC traces of G-TCTA and G-mCP at a heating rate of $10\text{ }^{\circ}\text{C min}^{-1}$; (b) AFM topographic images of G-TCTA and G-mCP.

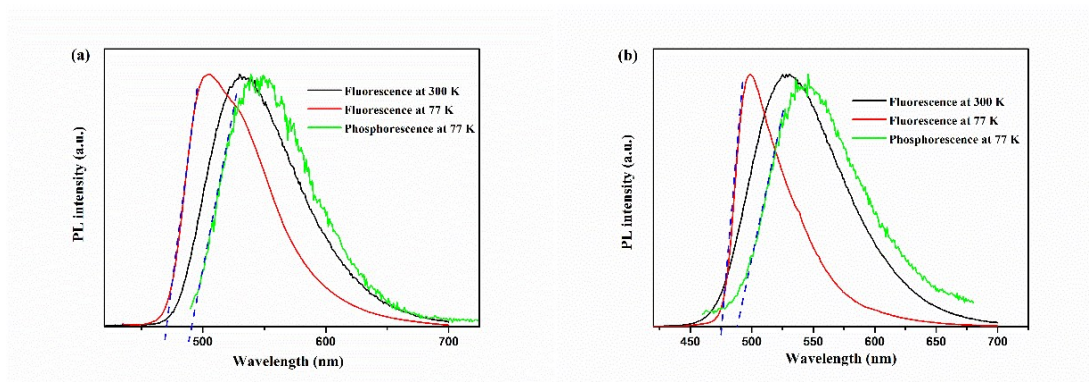


Fig. S11. Fluorescence and phosphorescence spectra of G-TCTA and G-mCP in toluene at 300K and 77 K.

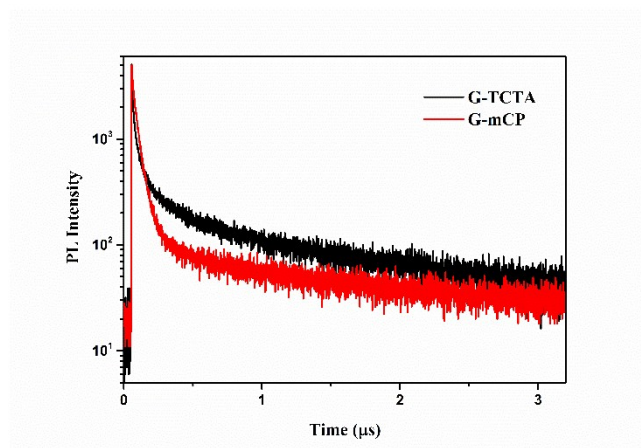


Fig. S12. Transient fluorescence decays of G-TCTA and G-mCP in films at 300 K.

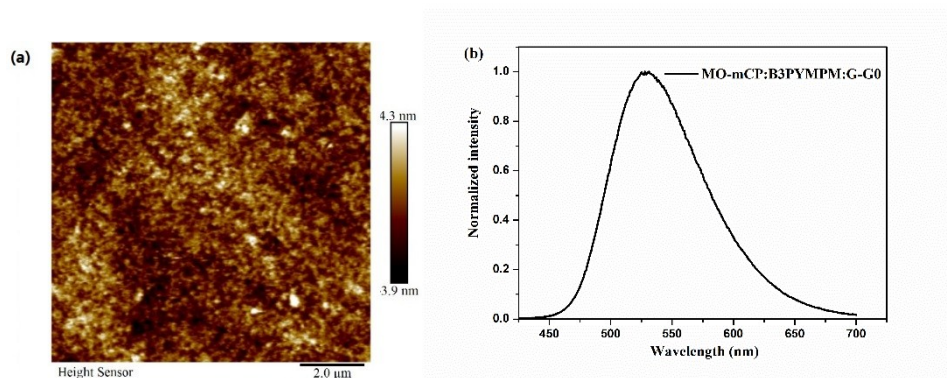


Fig. S13. (a) AFM topographic images of blending film MO-mCP: G-G0 (4:1); (b) Normalized PL spectra of MO-mCP: B3PYMPM: G-G0 (4: 4: 1) blended films.

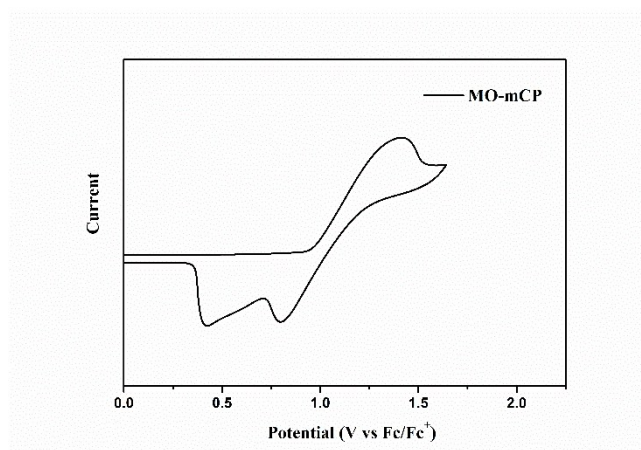


Fig. S14. Oxidation part of the CV curves of MO-mCP in dichloromethane.

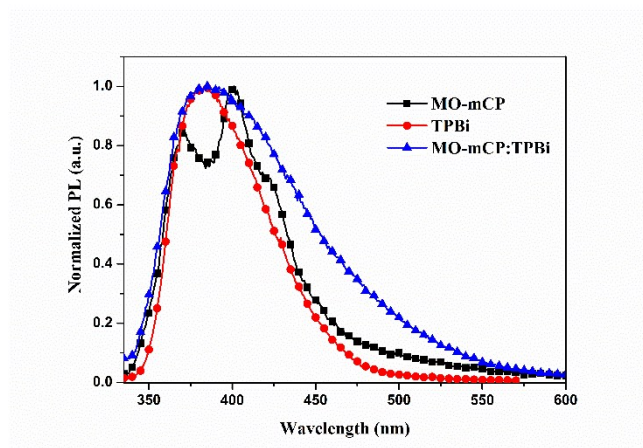


Fig. S15. Normalized PL spectra of MO-mCP, TPBi, and MO-mCP:TPBi (1:1, mol/mol) blended films.

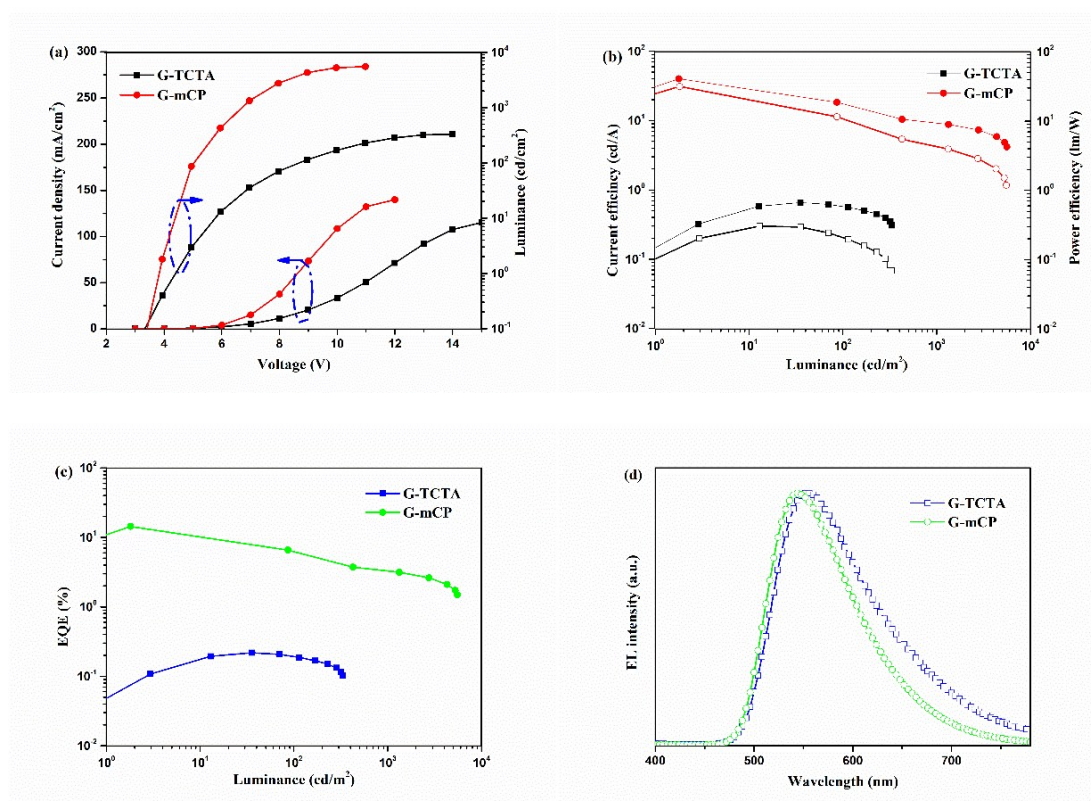


Fig. S16. The EL characteristics of devices based on G-TCTA and G-mCP. (a) Current density–voltage–brightness (J–V–L) characteristics. (b) Current efficiencies and power efficiencies versus brightness characteristics. (c) External quantum efficiencies versus brightness characteristics. (d) The EL spectra operated at 10 V.

Table S1. Comparison of solution-processed TADF OLEDs with vacuum-deposited ETL.

EML	V _{on} [V]	PE _{max} [lm W ⁻¹]	EQE _{max} [%]	CE _{max} [cd A ⁻¹]	L _{max} [cd m ⁻²]	CIE [x,y]	
G-mCP ^a	2.7	46.6	16.5	44.5	18800	(0.42,0.55)	This work
LEP ^a	/	/	10.0	/	/	(0.32,0.58)	Ref 1
PAPTC ^a	2.6	37.1	12.6	41.8	10251	(0.30,0.59)	Ref 2
P12 ^a	3.1	11.2	4.3	10.7	/	(0.24,0.43)	Ref 3
G3TAZ	3.5	/	3.4	/	/	(0.26,0.48)	Ref 20
CDE1 ^a	/	/	13.8	/	10000	(0.40,0.54)	Ref 21
2CzSO ^a	4.7	/	10.7	/	4706	/	Ref 22
CzDMAC-DPS ^a	3.6	24.0	12.2	30.6	/	(0.24,0.44)	Ref 23
G2B ^a	3.4	11.5	5.7	14.0	/	(0.26,0.48)	Ref 24
TZ-3Cz ^a	3.6	/	10.1	30.5	22000	(0.24,0.51)	Ref 25
POCz-DPS	5.4	/	12.6	7.3	2700	(0.18,0.30)	Ref 26
SiCz:t4CzIPN ^b	/	42.7	18.7	/	/	(0.31,0.59)	Ref 4
CBP:PXZDSO2 ^b	4.1	/	15.2	45.1	/	(0.42,0.55)	Ref 5
CBP:ACRDSO2 ^b	3.7	/	17.5	53.3	/	(0.32,0.58)	Ref 5
mCP:4CzCNPy ^b	4.7	14.8	11.3	38.9	/	(0.34,0.59)	Ref 6
SiCz:TB-3PXZ ^b	/	32.6	13.9	41.5	10000	(0.23,0.54)	Ref 7
CBP:4CzIPN ^b	3.4	/	18.5	/	/	(0.32,0.56)	Ref 8
TCTA:pAcBP ^b	/	20.3	9.3	31.8	30800	(0.38,0.57)	Ref 9
TCTA:pCzBP ^b	/	9.0	8.1	24.9	5100	(0.28,0.43)	Ref 9
PCzDP-10 ^b	/	14.1	16.1	38.6		(0.22,0.40)	Ref 10
mCP:Copo1 ^b	/	40.1	20.1	61.3	/	(0.36,0.55)	Ref 11

^a Non-doped device, ^b Doped device.